Appl Phys B (2011) 103:547–551
DOI 10.1007/s00340-010-4229-x

Applied Physics B
Lasers and Optics

Nanofabrication by magnetic focusing of supersonic beams

R.J. Clark · T.R. Mazur · A. Libson · M.G. Raizen

Received: 23 July 2010 / Published online: 17 September 2010

Abstract We present a new method for nanoscale atom lithography. We propose the use of a supersonic atomic beam, which provides an extremely high brightness and cold source of fast atoms. The atoms are to be focused onto a substrate using a thin magnetic film, into which apertures with widths on the order of 100 nm have been etched. Focused spot sizes near or below 10 nm, with focal lengths on the order of 10 μm, are predicted. Our method can be implemented in a highly parallel manner, enabling simultaneous fabrication of 10^6 identical elements, and it is applicable both to precision patterning of surfaces with metastable atomic beams and to direct deposition of material.

1 Introduction

Atom lithography is a novel approach to nanofabrication in which beams of atoms impinge on a surface and form structures thereon through optical, magnetic, or mask-based patterning [1, 2]. For some applications, it presents an interesting alternative to more common fabrication methods such as optical lithography, electron-beam lithography, and focused ion beam milling [3–5]. For instance, areas of fundamental research such as quantum photonics [6], plasmonics [7], and metamaterials [8] would benefit from fabrication methods which provide feature sizes on the scale of those obtained with electron or ion beams ($\mathcal{O}(10\,\text{nm})$), but with increased parallelism, meaning that a larger number of identical elements could be fabricated simultaneously. Atom lithography appears to be such a method. In principle, feature sizes can be smaller than those obtained by optical lithography, since the de Broglie wavelength of atoms is typically much less than an optical wavelength, resulting in a much smaller diffraction-limited spot size. Additionally, much work has been reported on depositing multiple lines and dots of atoms by focusing from a standing light wave [9–13], highlighting the potential parallelism of atom lithography. Several other developing techniques also aim to bridge this gap between parallelism and feature size, including extreme ultraviolet optical lithography [5, 14], ion projection lithography [15], and nanoimprint lithography [16]. Despite some impressive achievements, for instance obtaining 11 nm feature sizes with some degree of parallelism using ion projection lithography,[1] there are instances when neutral atom lithography may be a more suitable technique, especially for any class of device for which direct deposition is preferred to lithographic patterning, or whenever the damage caused to a surface by an energetic ion beam is unacceptable. Atom lithography is versatile in the sense that one may either directly write structures onto a substrate [17–21], or may pattern a resist prior to etching, as in traditional lithography, using a beam of metastable atoms [22].

Atom lithography, however, is not without significant challenges. As one example, the primary limitation of optical focusing is that it is difficult to focus some of the atoms without simultaneously defocusing others, leading to significant aberrations and an unwanted underlayer of material. A method of mitigating this effect was proposed [23] and demonstrated [24], but is challenging to implement in practice. Alternative approaches, such as focusing of atoms using macroscopic magnetic lenses [25–27] or an "atom pinhole camera" [28] have also been explored. However, experiments in atom lithography to date have achieved con-

R.J. Clark (✉) · T.R. Mazur · A. Libson · M.G. Raizen
Center for Nonlinear Dynamics and Department of Physics, The University of Texas at Austin, Austin, TX, 78712, USA
e-mail: robclark@physics.utexas.edu

[1] See, for instance http://www.charpan.com/index.html.

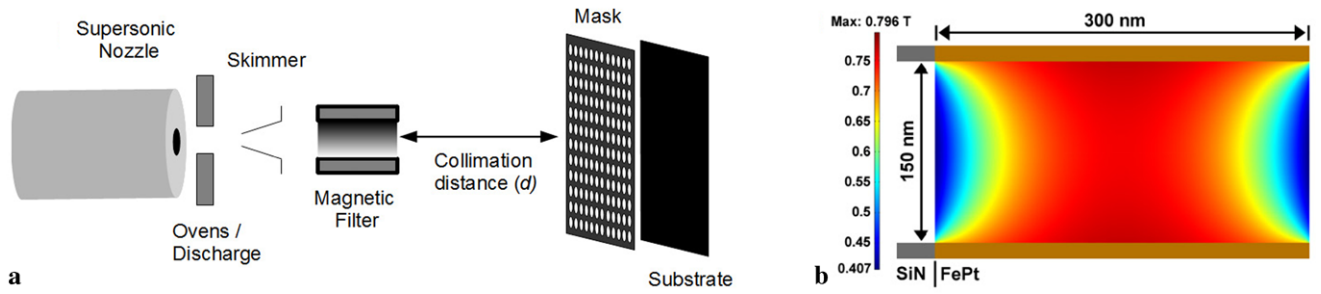

Fig. 1 (**a**) Schematic (not to scale) of our nanolithography process. The supersonic nozzle produces a bright atomic beam, which may either be excited to a metastable level in a discharge or have atoms entrained into it from some number of ovens. Following this, the beam is collimated by passing through a skimmer. Magnetic filtering ensures that only the correct m_J state arrives at the mask, which then focuses the atoms onto a substrate. (**b**) Schematic (not to scale) of a single hole in the mask with proposed dimensions given. A Si_3N_4 substrate supports a 300 nm-thick FePt mask with perpendicular magnetization of 670 kA/m. Only small regions of the mask and substrate are shown; the actual length of the substrate is on the order of 1 μm. The magnitude of the magnetic field within the hole in the mask is plotted

trolled feature sizes (at best) on the order of 100 nm, limited by aberrations from the focusing elements or by the limited collimation of the atomic beam. Furthermore, they have employed effusive atomic beams, limiting atomic density to around 10^{10} atoms/cm^3, which in turn limits the overall throughput of the technique.

In this article, we propose a new approach to atom lithography that, in principle, enables much smaller feature sizes and larger throughput. Our method consists of magnetic focusing of a supersonic beam through a microfabricated magnetic mask. As nearly all atoms are paramagnetic in either the ground state or an optically-accessible metastable state, magnetic focusing is a very general approach. Furthermore, the supersonic beam provides both high atomic flux and a low temperature $T \approx 100$ mK, a unique combination. This paper is organized as follows. In Sect. 2, we present details of our proposed method, including the supersonic source and focusing apparatus. Section 3 contains simulation results, including spot sizes and focal lengths for a number of atomic species. Finally, in Sect. 4, we discuss the scalability and potential applications of our method.

2 Apparatus

Our proposed apparatus (see Fig. 1) consists of two main components: a supersonic beam of spin-polarized atoms, and a thin magnetic mask into which an array of holes of $\mathcal{O}(100\text{ nm})$ width is etched, through which the atoms are focused onto a substrate. Depending on whether one wishes to deposit material or pattern using excited-state atoms, one either entrains atoms into the beam from one or more ovens, or excites the carrier gas to a metastable level in a discharge. The basic principle of our method is that the very high magnetic field gradients due to the tiny holes in the magnetic material will be able to focus atoms, even though they are traveling at hundreds of meters per second.

A continuous-wave supersonic beam [29, 30] will provide an atomic flux on the order of 10^{20} atoms/sr/s [31]. A typical fraction of either metastable or entrained atoms in the beam is 10^{-3}. Following a skimmer, atoms in a specific internal magnetic sublevel m_J will be selected by some method of magnetic filtering; either magnetic guiding or deflection may be used. Alternatively, optical pumping could be implemented on many atomic species. For some species, especially metastable noble gases, laser collimation (by transverse laser cooling) may be applied to increase the beam brightness by a factor of 10^3 or higher, while reducing the velocity spread in the radial direction [17, 32, 33].

The focusing mask consists of a thin film of a magnetized material, deposited on a substrate, with the magnetization vector pointing out of the plane of the film. Such a film (specifically, a 300 nm-thick FePt film) was recently used to build a permanent-magnet chip trap for atoms [34, 35]. Holes of diameter on the order of 100 nm will be etched into the film and into the substrate that supports it (Fig. 1). This substrate could be made of one of many materials, such as silicon nitride (Si_3N_4) or silicon, and may be as thick as several microns. The holes in both layers may be fabricated by e-beam or optical lithography, and may be arranged in any desired pattern; non-circular apertures may also be used. A hole-to-hole spacing of 1 μm should be sufficient to preserve the structural integrity of the mask.[2] Our method lends itself to highly parallel fabrication: given a conservative estimate for the diameter of the incident atom beam of 1 mm, roughly one million apertures can focus atoms simultaneously.

The atoms are focused by the force $\boldsymbol{F}$ due to the interaction of the atomic magnetic dipole moment $\boldsymbol{\mu}$ with the magnetic field $\boldsymbol{B}$ of the magnetized mask: $\boldsymbol{F} = \nabla(\boldsymbol{\mu} \cdot \boldsymbol{B})$. Assuming the atomic magnetic dipole adiabatically follows

[2] By way of comparison, a 0.5 μm thick transmission grating with a period of 0.2 μm has been used for atom diffraction experiments [36].

the magnetic field, we may write the force in the radial direction (normal to the propagation direction) as

$$F_r = -\mu_B g_J m_J \big(\partial |B| / \partial r\big), \tag{1}$$

where μ_B is the Bohr magneton and g_J is the Landé g-factor. For the simulations that follow, we assume a material thickness of 300 nm and a perpendicular magnetization of $M = 670$ kA/m (as reported in [34, 35]). We also choose a hole diameter of 150 nm, which is within the range of optical lithography, and a substrate thickness of 1 μm. The magnetic fields are computed numerically; the peak field near such a hole is $|B| \approx 0.8$ T, and a typical radial field gradient within the hole is $\partial |B| / \partial r = 1000$ T/cm (see Fig. 1).

To estimate the number of atoms that passes through each hole per unit time, as well as to estimate the spread in radial velocities, we use a simple model of geometric collimation. The efficiency ϵ represents the fraction of atoms emitted from a skimmer of radius r_s that will pass through the focusing aperture; it is calculated as the ratio of the area of the circular hole in the mask to the area of the atomic beam at the position of the mask. Writing the beam divergence angle as θ, the distance from the skimmer to the mask as d, and the radius of the hole as r_m, $\epsilon = r_m^2/(r_s + d\tan\theta)^2$. Typical numbers for our chosen conditions are $r_s = 125$ μm, $r_m = 75$ nm, $\theta = 7°$, and $d = 2$ m, leading to $\epsilon \approx 1 \times 10^{-13}$. Given the beam brightness of 10^{20} atoms/sr/s, a discharge or entrainment efficiency of 10^{-3}, and a loss of one in ten atoms due to magnetic filtering, we estimate a flux through each hole of $\approx 10^3$ atoms/s.

3 Simulations

The primary goal of our simulations is to calculate the focused spot sizes as the parameters of the problem, including the atomic species and the amount of collimation, are varied. Unless stated otherwise, we assume that the beam is moving with a center-of-mass speed of $v_0 = 400$ m/s, an appropriate value for a neon beam at 77 K. We also assume the radius of the (circular) skimmer is $r_s = 125$ μm. We assign each atom a random transverse velocity, due to geometric collimation, within the range $\Delta v_t \approx 2 r_s v_0 / d$, where d is the distance from the skimmer to the mask. The spread in velocities along the propagation axis Δv_z is a property of the beam that is due to the supersonic expansion (not to collimation). It is assumed, based on measurements in our laboratory, to be fixed at $\Delta v_z = 14$ m/s for neon at 77 K [37]. Simulations are performed by numerically integrating the equations of motion for a particle moving through the hole in the mask. The spot size w_0 is calculated as twice the average value $\langle r \rangle$ of the radius of atoms at the focal point, weighted by the density of atoms at a given radius:

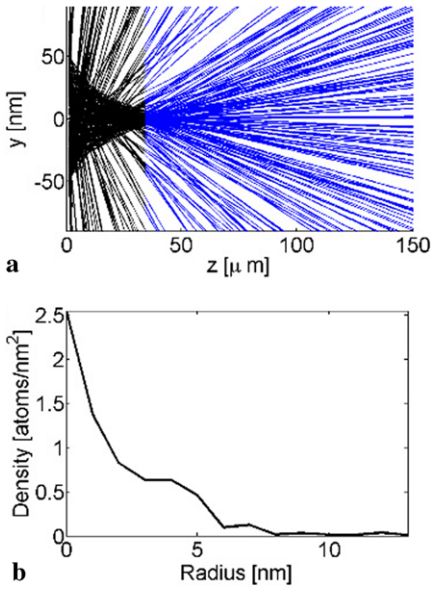

Fig. 2 (**a**) Cross-section of 250 trajectories for ^{20}Ne with a center-of-mass speed of 400 m/s and a collimation distance of $d = 2$ m. The front face of the mask is located on $z = 0$, and the center of the hole lies on $r = 0$. The spot size $w_0 = 8.5$ nm and the focal length $f = 34$ μm. The color of the trajectories changes from *black* to *blue* at the *focal plane*. This spot size is less than the diffraction-limited spot size $w_d = 11.1$ nm; the true spot size will be the result of the convolution of an Airy disc of FWHM w_d with the distribution of atoms found via ray tracing. (**b**) Density of atoms as a function of radius at the focal point for the data in (**a**)

$\langle r \rangle = \int (\rho(r)\, r\, dr) / \int (\rho(r)\, dr)$, where $\rho(r)$ is the density of atoms at radius r and the integral is evaluated discretely using $dr = 1$ nm.

We present simulation results in Fig. 2 showing focusing of metastable neon. Even when many atoms reach the substrate far from $\langle r \rangle$, the density of atoms there is orders of magnitude less than near the focus. There are two dominant mechanisms, apart from limited collimation, by which the spot is broadened: aberrations, and van der Waals attractions within the substrate and mask. Aberrations appear in the numerical solution to the fields within the mask. Van der Waals forces are modeled by including a force term in the equations of motion that was calculated numerically and is well-approximated as being proportional to $D_2^{-4} - D_1^{-4}$, where D_2 is the distance to the nearest edge of the tube and D_1 the distance to the furthest edge. For atoms that are close enough to the wall of the tube, this force either causes the atom to collide with the tube or to strike the substrate far from the focused spot. Atoms that strike the tube walls are removed from the simulation, because they will, with high probability, either release their internal energy, making them ineffective for patterning, or scatter inelastically and not be focused. Although we obtain a simulated spot size of $w_0 = 8.5$ nm, the diffraction-limited spot size w_d for our parameters is $w_d = 1.03 \lambda_{\mathrm{dB}} f/(2 r_m) = 11.1$ nm, where the de Broglie wavelength $\lambda_{\mathrm{dB}} = h/(mv) \approx 0.25$ nm, and w_d is

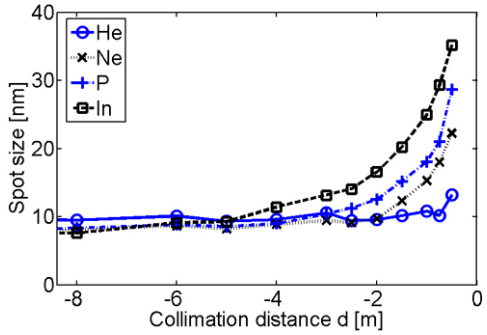

Fig. 3 Simulated spot size w_0 as a function of collimation distance d for four atomic species. All species except phosphorus are in a metastable excited state (given in Table 1). These large-d spot sizes are smaller than the diffraction-limited spot sizes, also reported in Table 1. Helium has the largest spot size at large d because it is affected more, due to its low mass, by van der Waals forces, while at small d, the spot is smaller due to its relatively high ratio of magnetic moment to mass

taken to be the full width at half-maximum (FWHM) of the Airy disc. Therefore, our simulations suggest that we can focus to a diffraction-limited spot size.

Highlighting the generality of our method, our simulations show that the same mask can focus a very wide range of atomic masses with spot sizes of $\mathcal{O}(10\,\text{nm})$. Figure 3 shows the spot sizes as a function of collimation distance d. For low d, the radial velocity spread dominates, while for high d, van der Waals forces and aberrations dominate. In Table 1, we report the expected spot size and focal length for several species of interest at a fixed value of $d = 2$ m. For some atoms, laser excitation at a single frequency will be necessary, since they are either non-paramagnetic or have too small a magnetic moment in the ground state or discharge-induced metastable state. For these species, a single photon will suffice to pump the atom (with some probability) into a suitable metastable state, which must have a lifetime larger than the time it takes for the atom to be deposited (typically a few milliseconds). Two notable examples are indium and gallium, which each occupy a $^2\text{P}_{1/2}$ ground state, with maximal magnetic moment $\mu_B/3$. A single photon, at 410 nm for In and at 403 nm for Ga, would pump the atoms to a metastable $^2\text{P}_{3/2}$ state, with maximal magnetic moment $6\mu_B$, a state that is focused very well. The branching ratio into the desired state is 38% for In and 67% for Ga.[3] Although there is some possibility that non-noble gas species will clog the apertures, we note that clogging was not reported to be an issue in the work of [36].

[3]Atomic data taken from the NIST Handbook of Basic Atomic Spectroscopic Data, http://www.nist.gov/physlab/data/handbook/index.cfm.

Table 1 Spot sizes (w_0) and focal lengths (f) for a variety of species. All are traveling at 400 m/s and have traversed 2 m following a 250 μm skimmer. The approximate diffraction-limited spot size w_d is also given; the actual spot size is expected to be the convolution of the atomic distribution of waist w_0 and the Airy disc of FWHM w_d. The magnetic moment ($|\boldsymbol{\mu}|$), and atomic state are given for reference. All except ^{31}P are in metastable states. The width of both the substrate and the mask is 150 μm

Species	$\lvert\boldsymbol{\mu}\rvert$ (μ_B)	w_0 (nm)	w_d (nm)	f (μm)	State
^{4}He	2	8.5	12.3	7.2	$^3\text{S}_1$
^{20}Ne	3	10.0	11.1	32.6	$^3\text{P}_2$
^{31}P	3	12.1	9.9	44.6	$^4\text{S}_{3/2}$
^{70}Ga	6	11.7	5.2	53.7	$^2\text{P}_{3/2}$
^{114}In	6	17.1	5.0	82.3	$^2\text{P}_{3/2}$

4 Discussion

Our simulations indicate that, for a wide variety of atomic species, focusing to spot sizes on the order of 10 nm may be achieved with the apparatus presented in Sect. 2. In fact, the spot size is limited by diffraction from the mask aperture for several of the species we examined. Since the FWHM of the Airy disc is given by $w_d = 1.03\lambda_{\text{dB}} f/(2r_m)$, a decrease in the ratio f/r_m will reduce the diffraction limit. Simulations with multiple layers of thin film magnetic material show a decreased focal length with identical mask apertures, resulting in a smaller diffraction limit with similar or better spot sizes. Alternatively, advances in the thin film magnetic materials may provide for greater magnetizations, which would similarly reduce the focal length. As such, we do not regard the calculated diffraction limits for our simulated apparatus as being the best that can be achieved with this method.

Among the many potential applications of our method, one of the most intriguing is the fabrication of quantum dots. Currently, quantum dots are most frequently fabricated by molecular beam epitaxy, which results in quantum dots of random size and location. Our scheme could produce dots with a position known to within a few nm and a size limited only by the Poisson fluctuations. Mounting the mask on a nanometer-resolution translation stage increases the versatility of our method. For instance, the quantum dots could be combined with nanofabricated wires or mirrors, producing electrical or optical interconnects between the dots. This could enable one vision of quantum computation with quantum dots [38, 39]. Our method has many other potential uses, as well: applications to basic science include plasmonics [7], metamaterials [8], and quantum photonics [6], while applications of commercial interest include photovoltaics, light sources, and light sensors.

In conclusion, we have outlined a new method for fabricating a wide variety of nanoscale devices with an unprecedented combination of nanometer precision and high throughput. Our method relies on technologies that are well

understood, including supersonic beams and magnetic filtering, and has no strenuous laser requirements. The required magnetic mask is based on readily-available magnetic thin film and lithographic technology and affords the possibility of writing $\mathcal{O}(10^6)$ identical elements in parallel. Our method should open up new possibilities in the fabrication of nanoscale semiconductor quantum devices, including light sources and detectors, plasmonic devices, and quantum information processors.

Acknowledgements We gratefully acknowledge fruitful discussions with Dan Ralph, David Sellmyer, Andrew Houck, Walt de Heer, and Rene Gerritsma, and funding from the Sid W. Richardson Foundation and the R. A. Welch Foundation, grant number F-1258.

References

1. D. Meschede, H. Metcalf, J. Phys. D **36**, R17 (2003)
2. V.I. Balykin, P.N. Melent'ev, Nanotechnol. Russ. **4**, 425 (2009)
3. P. Rai-Choudhury (ed.), *Handbook of Microlithography, Micromachining, and Microfabrication* (SPIE Optical Engineering Press and the Institution of Electrical Engineers, Bellingham, 1997)
4. L.A. Giannuzzi, F.A. Stevie (eds.), *Introduction to Focused Ion Beams: Instrumentation, Theory, Techniques and Practice* (Springer, Berlin, 2005)
5. B. Wu, A. Kumar, *Extreme Ultraviolet Lithography* (McGraw-Hill, Bellingham, 2009)
6. J.L. O'Brien, A. Furusawa, J. Vuckovic, Nature Photonics **3**, 687 (2009)
7. J.A. Schuller, E.S. Barnard, W. Cai, Y.C. Jun, J.S. White, M.L. Brongersma, Nature Mater. **9**, 193 (2010)
8. V.M. Shalaev, Nature Photonics **1**, 41 (2007)
9. K.S. Johnson, J.H. Thywissen, N.H. Dekker, K.K. Berggren, A.P. Chu, R. Younkin, M. Prentiss, Science **280**, 1583 (1998)
10. M. Baker, A.J. Palmer, W.R. MacGillivray, R.T. Sang, Nanotechnology **15**, 1356 (2004)
11. W. Lu, K.G.H. Baldwin, M.D. Hoogerland, S.J. Buckman, T.J. Senden, T.E. Sheridan, R.W. Boswell, J. Vac. Sci. Technol. B **16**, 3846 (1998)
12. A. Bard, K.K. Berggren, J.L. Wilbur, J.D. Gillaspy, S.L. Rolston, J.J. McClelland, W.D. Phillips, M. Prentiss, G.M. Whitesides, J. Vac. Sci. Technol. B **15**, 1805 (1997)
13. P. Engels, S. Salewski, H. Levsen, K. Sengstock, W. Ertmer, Appl. Phys. B **69**, 407 (1999)
14. Y. Chen, A. Pépin, Electrophoresis **22**, 187 (2001)
15. A.A. Tseng, Small **1**, 594 (2005)
16. S.Y. Chou, P.R. Krauss, P.J. Renstrom, Science **272**, 85 (1996)
17. J.J. McClelland, R.E. Scholten, E.C. Palm, R.J. Celotta, Science **262**, 877 (1993)
18. G. Timp, R.E. Behringer, D.M. Tennant, J.E. Cunningham, M. Prentiss, K.K. Berggren, Phys. Rev. Lett. **69**, 1636 (1992)
19. V. Natarajan, R.E. Behringer, G. Timp, Phys. Rev. A **53**, 4381 (1996)
20. R. Gupta, J.J. McClelland, Z.J. Jabbour, R.J. Celotta, Appl. Phys. Lett. **67**, 1378 (1995)
21. B. Smeets, P. van der Staten, T. Meijer, C.G.C.H.M. Fabrie, K.A.H. van Leeuwen, Appl. Phys. B **98**, 697 (2009)
22. K.K. Berggren, A. Bard, J.L. Wilbur, J.D. Gillaspy, A.G. Helg, J.J. McClelland, S.L. Rolston, W.D. Phillips, M. Prentiss, G.M. Whitesides, Science **269**, 1255 (1995)
23. I.S. Averbukh, R. Arvieu, Phys. Rev. Lett. **87**, 163601 (2001)
24. W.H. Oskay, D.A. Steck, M.G. Raizen, Phys. Rev. Lett. **89**, 163601 (2002)
25. W.G. Känders, F. Lison, A. Richter, R. Wynands, D. Meschede, Nature **375**, 214 (1995)
26. W.G. Kaenders, F. Lison, I. Müller, A. Richter, R. Wynands, D. Meschede, Phys. Rev. A **54**, 5067 (1995)
27. R.R. Chaustowski, V.Y.F. Leung, K.G.H. Baldwin, Appl. Phys. B **86**, 491 (2007)
28. P.N. Melentiev, A.V. Zablotskiy, D.A. Lapshin, E.P. Sheshin, A.S. Baturin, V.I. Balykin, Nanotechnology **20**, 235301 (2009)
29. R. Campargue (ed.), *Atom and Molecular Beams: The State of the Art 2000* (Springer, Berlin, 2001)
30. H. Pauly, *Atom, Molecule and Clusterbeams I: Basic Theory, Production, and Detection of Thermal Energy Beams* (Springer, Berlin, 2000)
31. J.R. Buckland, Ph.D. thesis, University of Cambridge, Cambridge, UK (1998)
32. M.D. Hoogerland, J.P.J. Driessen, E.J.D. Vredenbregt, H.J.L. Megens, M.P. Schuwer, H.C.W. Beijerinck, K.A.H. van Leeuwen, in *Proceedings of the 1994 IEEE International Frequency Control Symposium* (IEEE, New York, 1994), p. 651
33. E. Rasel, F.P.D. Santos, F.S. Pavone, F. Perales, C.S. Unnikrishnan, M. Leduc, Eur. J. Phys. D **7**, 311 (1999)
34. Y.T. Xing, I. Barb, R. Gerritsma, R.J.C. Spreeuw, H. Luigjes, Q.F. Xiao, C. R'etif, J.B. Goedkoop, J. Magn. Magn. Mater. **313**, 192 (2007)
35. T. Fernholz, R. Gerritsma, S. Whitlock, I. Barb, R.J.C. Spreeuw, Phys. Rev. A **77**, 033409 (2008)
36. D.W. Keith, M.L. Schattenburg, H.I. Smith, D.E. Pritchard, Phys. Rev. Lett. **61**, 1580 (1988)
37. E. Narevicius, A. Libson, C.G. Parthey, I. Chavez, J. Narevicius, U. Even, M.G. Raizen, Phys. Rev. Lett. **100**, 093003 (2008)
38. D. Loss, D.P. DiVincenzo, Phys. Rev. A **57**, 120 (1998)
39. A. Imamoglu, D.D. Awschalom, G. Burkard, D.P. DiVincenzo, D. Loss, M. Sherwin, Phys. Rev. Lett. **83**, 4204 (1999)